# A MODEL STUDY OF INTRACELLULAR OXYGEN GRADIENTS IN A MYOGLOBIN-CONTAINING SKELETAL MUSCLE FIBER

WILLIAM J. FEDERSPIEL
*Department of Biomedical Engineering, The Johns Hopkins School of Medicine, Baltimore, Maryland 21205*

ABSTRACT A theoretical two-dimensional model is used to investigate oxygen gradients in a red skeletal muscle fiber. The model describes the steady state, free and myoglobin-facilitated diffusion of oxygen into a respiring cylindrical muscle fiber cross section. The oxygen tension at the sarcolemma is assumed to vary along the sarcolemma as an approximation to the discrete capillary oxygen supply around the fiber. Maximal oxygen gradients are studied by considering parameters relevant to a maximally-respiring red muscle fiber. The model predicts that angular variations in the oxygen tension imposed at the sarcolemma due to the discrete capillary sources do not penetrate deeply into the fiber over a range of physiological values for myoglobin concentration, diffusion coefficients, number of surrounding capillaries, and oxygen tension level at the sarcolemma. Also, the oxygen tension in the core of the fiber is determined by the average oxygen tension at the sarcolemma. The drop in oxygen tension from fiber periphery to core, however, does depend significantly on the myoglobin concentration, the oxygen tension level at the sarcolemma, and the oxygen and myoglobin diffusivities. This dependence is summarized by calculating the minimum average sarcolemmal oxygen tension for maximal respiration without the development of an intracellular anoxic region. For a myoglobin-rich muscle fiber (0.5 mM myoglobin), the model predicts that maximal oxygen consumption can proceed with a relatively flat (<5 mm Hg) oxygen tension drop from fiber periphery to core over a large range for diffusion coefficients.

## INTRODUCTION

The magnitude of intracellular gradients of oxygen tension in red muscle fibers and the in-situ role of the heme protein myoglobin as a facilitator for oxygen transport are directly related questions that are not completely resolved. A prerequisite for myoglobin-facilitated oxygen transport in red muscle fibers is a gradient in the oxygen saturation of myoglobin (see the reviews by Wittenberg, 1970; Kreuzer, 1970; and Jacquez, 1984), and this in turn requires that the oxygen tension of the fiber be low enough so that myoglobin is only partially saturated with oxygen. Under these conditions, myoglobin can facilitate the transport of oxygen in red muscle tissue, as has been demonstrated in experiments using isolated bundles of unperfused pigeon breast muscle (Wittenberg et al., 1975) and slices of chicken gizzard smooth muscle (Koning et al., 1981). Cole (1982) found that oxygen tension and twitch tension generation were compromised when functional myoglobin was abolished in the perfused, isolated dog gastrocnemius-plantaris muscle, thus implying that myoglobin was acting as a transport facilitator for oxygen before its function was abolished. Jones and Kennedy (1982), however, concluded from their studies on isolated cardiac myocytes that the oxygen concentration gradient from sarcolemma to mitochondria is very large during normal respiratory activity of the cell and that myoglobin does not significantly facilitate the transport of oxygen from sarcolemma to mitochondria. Measurements of oxygen tension in exercising dog gracilis muscle (Gayeski and Honig, 1983; Honig et al., 1984), obtained using the myoglobin cryomicrospectrophotometric technique, indicate that the oxygen tension is low (<3 mm Hg) and that the oxygen tension variation within a fiber is relatively small (~1 mm Hg) during maximal and near-maximal oxygen consumption.

In this study, a steady-state two-dimensional model of oxygen diffusion into a myoglobin-containing muscle fiber is used to specifically analyze the magnitude of oxygen tension gradients in a single red muscle fiber. Earlier model studies concentrated primarily on elucidating the mechanisms of myoglobin-facilitated oxygen transport in muscle fibers. Wyman (1966) modeled the steady-state one-dimensional oxygen diffusion into a cylindrical muscle fiber containing myoglobin and surrounded by a uniform oxygen tension at the sarcolemma; Wyman showed that myoglobin can carry a large fraction of the oxygen flow into the fiber by translational diffusion of oxymyoglobin molecules. Murray (1974) and Taylor and Murray (1977) extended Wyman's one-dimensional model by quantifying

William Federspiel's present address is the Biomechanics Institute, 896 Beacon Street, Boston, Massachusetts 02215

the oxygen concentration and myoglobin saturation gradients as functions of oxygen consumption. Model studies have also looked at myoglobin-facilitated oxygen transport into tissue using a Krogh cylinder idealization of tissue (cf. Fletcher, 1980) in order to introduce more-realistic interactions with blood flow and oxygen supply. Since myoglobin cannot diffuse freely across muscle cell (fiber) boundaries, however, the Krogh formulation (a capillary surrounded by several muscle fibers) may not be as appropriate as a single muscle fiber model for studying intracellular gradients (Jacquez, 1984). The present study extends the earlier single-fiber work by considering an elementary two-dimensional model relevant to the question of the magnitude of oxygen gradients in single red muscle fibers in situ. In addition, the specific effect of myoglobin concentration is considered. Despite the simplicity of the model, several important concepts about oxygen gradients in skeletal muscle fibers can be learned from it.

Consider a simple description of the process being modeled. The perpendicular cross section of a skeletal muscle fiber in Fig. 1 is supplied oxygen from several perfused, surrounding capillaries, that also supply oxygen to contiguous fibers. In very general terms, at the level of a single fiber cross section, oxygen tension gradients in two directions may arise: a gradient from fiber periphery to core required to supply oxygen to the center of the fiber; and an "angular" gradient at the fiber periphery due to the discrete capillary sources around the fiber. Though the extent of the latter gradient in-vivo is not known from experiments, a principal conclusion of this study is that it does not persist deeply into the fiber for physiologically relevant conditions. Also, the oxygen tension drop from periphery to core can be very small without compromising maximal oxygen consumption provided that the myoglobin concentration of the fiber exceeds 0.1 mM and the diffusion coefficients for oxygen and myoglobin are at the upper portion of the physiological range. These concepts are summarized by defining the minimum average oxygen tension at the periphery of a muscle fiber that is required for maintaining maximal oxygen consumption without developing an anoxic core in the fiber; this minimum oxygen tension is presented as a function of myoglobin concentration.

## THE MATHEMATICAL MODEL

### Descriptive Equations

The skeletal muscle fiber is modeled as a long right cylinder of radius $R$ with a polar coordinate system $(r, \theta)$ centered in the plane of the perpendicular cross section of the cylinder, as in Fig. 1. The length of the fiber is much greater than its diameter so that axial transport can be ignored, and only transport in an $r, \theta$ cross section is considered (Murray, 1974; Taylor and Murray, 1977). The chemical composition of interest is specified by the molar concentrations (moles/volume) of free (dissolved) oxygen, $N_1$, oxymyolobin, $N_2$, and free or unbound myoglobin, $N_3$. One can assume, however, that the total myoglobin concentration, $N_T = N_2 + N_3$, is spatially uniform and constant; thus the chemical compositions, $N_1$ and $N_2$, alone, are sufficient to characterize the system (Snell, 1965).

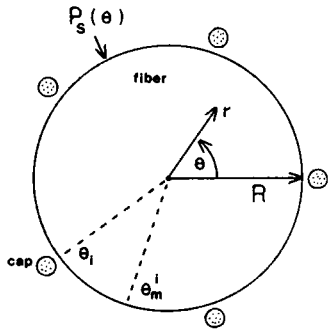


FIGURE 1 Two dimensional $(r, \theta)$ model of oxygen diffusion into a myoglobin-containing skeletal muscle fiber. The evenly spaced capillaries are located at the $\theta_i$ angular positions and the midcapillary angular positions are the $\theta_m^i$. The oxygen tension at the sarcolemma, $P_s(\theta)$, varies along the sarcolemma to model the discrete capillary oxygen supply.

At steady state the chemical composition in the muscle fiber is determined by a balance of molecular diffusion, chemical reaction between oxygen and myoglobin, and oxygen consumption. The differential mass conservation laws for oxygen and oxymyoglobin that express this balance, assuming constant diffusivities, $D_1$ and $D_2$ for oxygen and oxymyoglobin, are:

$$0 = D_1\nabla^2 N_1 - T - M \tag{1}$$

$$0 = D_2\nabla^2 N_2 + T, \tag{2}$$

where $T$ is the net rate of the reaction between oxygen and myoglobin to form oxymyoglobin (moles/volume/time), $M$ is the oxygen consumption rate (moles/volume/time), and $\nabla^2$ is the Laplacian in polar coordinates:

$$\nabla^2 = 1/r\,\partial/\partial r\,(r\,\partial/\partial r) + 1/r^2\,\partial^2/\partial\theta^2. \tag{3}$$

The reversible binding reaction between oxygen and myoglobin,

$$O_2 + Mb \rightleftharpoons MbO_2, \tag{4}$$

is assumed to follow mass action kinetics. Thus, the net rate of the reaction from left to right in Eq. 4, $T$, can be expressed as

$$T = k_{-1}N_1N_3 - kN_2, \tag{5}$$

where $k_{-1}$ and $k$ are the association and dissociation reaction rate constants, respectively, that are available from experimental data. Eq. 5 is given most conveniently by introducing $N_{50}$, the molar concentration of free oxygen that saturates 50% of the myoglobin at equilibrium, and using the equilibrium relation, $N_{50} = k/k_{-1}$, to rewrite Eq. 5:

$$T = k\,[N_{50}^{-1}N_1\,(N_T - N_2) - N_2]. \tag{6}$$

The expression, $T$, models the reaction kinetics between myoglobin and oxygen and is included to avoid the need to assume a-priori that oxygen and myoglobin are in equilibrium. Thus, the transport equations are not forced to equilibrium, and their departure from equilibrium is discussed briefly in Results and Discussion.

In subsequent discussions we will refer to oxygen tension (partial pressure), $P$, and myoglobin saturation, $S$, rather than the molar concentrations of free oxygen and oxymyoglobin, respectively. The relations, $N_1 = \alpha P$ and $N_2 = N_TS$, where $\alpha$ is the oxygen solubility coefficient (assumed spatially uniform in the fiber), can then be used to derive the final form of the steady-state transport equations:

$$0 = \alpha D_1\nabla^2 P - T^* - M \tag{7}$$

$$0 = D_2\nabla^2 S + N_T^{-1}T^*, \tag{8}$$

where

$$T^* = kN_T [P_{50}^{-1}P(1 - S) - S]. \quad (9)$$

$P_{50}$ is the oxygen tension saturating 50% of the myoglobin at equilibrium and is related to $N_{50}$ through the solubility of oxygen, $N_{50} = \alpha P_{50}$.

The solution to the transport equations, Eqs. 7 and 8, subject to the boundary conditions discussed in the next section is obtained using numerical methods. These methods are outlined in the Appendix, where in addition, typical oxygen tension profiles showing proper convergence of the numerical results are presented.

## Boundary Conditions

The supply of oxygen to a single muscle fiber from blood flowing through the surrounding capillaries is very complex. Thus, we select the simplest boundary condition relevant to the question of intracellular oxygen gradients. At the sarcolemma of the muscle fiber, $r = R$, the oxygen tension is specified, i.e. $P(r = R, \theta) = P_s(\theta)$. The sarcolemmal oxygen tension, $P_s(\theta)$, is assumed to vary along the sarcolemma as an approximation to the discrete capillary oxygen supply around the fiber (see Fig. 1).

To define $P_s(\theta)$ precisely is difficult because it is determined by a complicated balance of transport inside the fiber and oxygen supply from the discrete capillaries. In addition, there are no experimental data available as a guide in selecting $P_s(\theta)$. We begin by considering the case of similar capillaries spaced evenly around the fiber. This is clearly a simplification of the in-vivo situation, but the final results of the model suggest that a more elaborate treatment of this boundary condition would add little additional insight into what we can learn from the simpler boundary condition. To proceed, we assume $P_s(\theta)$ varies between some maximal value, $P_{max}$, and some minimal value, $P_{min}$, along the sarcolemma, where the maximal values occur adjacent to the capillaries and the minimal values occur midway between the capillaries. While this is a reasonable assumption, we do not know how $P_s(\theta)$ varies between $P_{max}$ and $P_{min}$ nor the exact relationship between $P_{max}$ and $P_{min}$. The simplest choice is a linear variation in $P_s(\theta)$ given by

$$P_s(\theta) = P_{min} + (P_{max} - P_{min}) |\theta_m^i - \theta| / (\theta_m^i - \theta_i)$$
$$\text{for } \theta_i \le \theta \le \theta_{i+1} \text{ and } i = 1, 2, \ldots C_f, \quad (10)$$

where $\theta_i$ denotes the angular locations of the capillaries, $\theta_m^i$ denotes the angular locations midway between capillaries, $C_f$ is the number of capillaries surrounding the fiber ($C_f$ is 5 in Fig. 1), and $||$ denotes the absolute value. Since appropriate values for $P_{max}$ and $P_{min}$ are not known precisely, calculations are done over a reasonable range of values for these parameters. Although it may be argued that in vivo the variation in $P_s(\theta)$ is not linear (as in Eq. 10), our primary interest is to introduce some variation in $P_s(\theta)$. The results of the calculations show that the major conclusions of the analysis are not sensitive to the particular form that the variation takes. Results of calculations based on quadratic and sinusoidal variations are essentially the same as the results based on the linear variation. (See Results and Discussion.)

The boundary condition for oxymyoglobin assumes that the sarcolemma is impermeable to oxymyoglobin since it is a large protein molecule. Thus, we have a no-flux condition:

$$\partial S / \partial r \, (r = R, \theta) = 0. \quad (11)$$

Eq. 11 represents the true boundary condition for oxymyoglobin. The oxymyoglobin saturation cannot be directly specified at the sarcolemma but rather is determined as part of the solution.

## Parameter Values

As an application of the model, we consider parameters relevant to maximally-respiring dog gracilis muscle, since the oxygen tension distribution has been studied experimentally in these muscles (Gayeski and Honig, 1983; Honig et al., 1984). In dog gracilis during maximal twitch exercise, oxygen consumption is relatively high, and thus the calculations presented here represent a special case in which one would expect the greatest oxygen concentration gradients to occur.

The most difficult parameters to assign are the diffusion coefficients for oxygen and oxymyoglobin in skeletal muscle. We are forced to define an appropriate range for these parameters from limited measurements of free oxygen diffusivity in muscle and other tissues in situ and from myoglobin diffusivity in in-vitro solutions. It is important to realize that many of the values reported in the literature for diffusion coefficients are measured at 20°C, or some other temperature below physiological, and must be corrected to 37°C (see Jacquez, 1984, for discussion on the temperature correction). For the free oxygen diffusion coefficient, $D_1$, some values available in the literature are: Krogh's original measurements (Wittenberg, 1970) for frog skeletal muscle, $1.3 \times 10^{-5}$ cm$^2$s$^{-1}$ at 20°C or $2.0 \times 10^{-5}$ cm$^2$s$^{-1}$ corrected to 37°C; MacDougall and McCabe (1967) for rat liver, $3.6 \times 10^{-5}$ cm$^2$s$^{-1}$ at 37°C; Kawashiro et al. (1975) for rat abdominal muscle, $1.6 \times 10^{-5}$ cm$^2$s$^{-1}$ at 37°C; and Ellsworth and Pittman (1984) for hamster soleus, $2.6 \times 10^{-5}$ cm$^2$s$^{-1}$, hamster retractor, $1.4 \times 10^{-5}$cm$^2$ s$^{-1}$, and hamster sartorius, $1.2 \times 10^{-5}$ cm$^2$s$^{-1}$, all at 37°C. This list, though not exhaustive, shows the range of possible values for the oxygen diffusion coefficient in tissues. Thus, a baseline (b) value is selected for the free oxygen diffusivity of $D_{1b} = 2 \times 10^{-5}$ cm$^2$s$^{-1}$, and results are presented below for a range of $D_1 = 1.5\ D_{1b}$, $D_{1b}$, $D_{1b}/2$, and $D_{1b}/3$.

The diffusion coefficient for myoglobin or oxymyoglobin has been predominantly measured in in-vitro solutions, but a value has recently been reported for in-situ bovine heart muscle of one-half its value in dilute buffer solution, or $\sim 1 \times 10^{-6}$ cm$^2$s$^{-1}$ (Livingston et al., 1983). For lack of experimental data on the diffusion coefficient for myoglobin in situ, we will assume that the ratio of the diffusivities of free oxygen and myoglobin is constant, i.e. independent of the diffusing medium, and we select a value for myoglobin diffusivity measured in a protein medium for which the free oxygen diffusivity is known. Riveros-Moreno and Wittenberg (1972) present values for myoglobin diffusivity in protein buffer ranging from $1.6 \times 10^{-6}$ cm$^2$s$^{-1}$ (dilute, corrected to 37°C) to $1.4 \times 10^{-6}$ cm$^2$s$^{-1}$ (10 g% protein, corrected to 37°C). Since free oxygen diffusivity is $\sim 2 \times$

TABLE I
MODEL PARAMETERS

| | | |
|---|---|---|
| $R$ | muscle fiber radius | 25 $\mu$m |
| $P_{50}$ | myoglobin equilibrium parameter | 5.3 mm Hg |
| $N_T$ | total myoglobin concentration | 0.5 mM (0.01–1.0)* |
| $M_{max}$ | oxygen consumption (maximal) | 15 ml $O_2$ 100 g$^{-1}$min$^{-1}$ |
| $D_1$ | oxygen diffusivity | $2.0 \times 10^{-5}$ cm$^2$s$^{-1}$ ($0.67–3.0 \times 10^{-5}$)* |
| $D_2$ | oxymyoglobin diffusivity | $1.5 \times 10^{-6}$ cm$^2$s$^{-1}$ ($0.5–2.3 \times 10^{-6}$)*‡ |
| $\alpha$ | oxygen solubility | $1.35 \times 10^{-9}$ mole cm$^{-3}$mm Hg$^{-1}$ |
| $k$ | dissociation rate constant | 66 s$^{-1}$ |
| $C_f$ | number of surrounding capillaries | 5 (3–5)* |
| $P_{max}/P_{50}$ | normalized maximum oxygen tension at sarcolemma | 2 (1–4)* |
| $P_{min}/P_{50}$ | normalized minimum oxygen tension at sarcolemma | 1 (0.1–2)* |

*Values in parentheses signify the range of the parameter considered, while the subscript "b" used in text refers to the baseline value.
‡The ratio, $D_2/D_1$, is fixed at 0.075 in all calculations.

$10^{-5}$ cm$^2$s$^{-1}$ in protein buffer of about 10 g% (Goldstick et al., 1975), we select a ratio for $D_2/D_1$ of $(1.5 \times 10^{-6})/(2 \times 10^{-5}) = 0.075$. Thus, the range for $D_2$ is related to that for $D_1$ above with $D_2/D_1$ fixed at 0.075. In absolute terms the ranges for $D_1$ and $D_2$ in cm$^2$s$^{-1}$ used in this study are $3 \times 10^{-5} \leq D_1 \leq 6.7 \times 10^{-6}$ and $2.3 \times 10^{-6} \leq D_2 \leq 5.0 \times 10^{-7}$. These ranges are consistent with values used in previous model studies. The assumption of a fixed ratio for $D_2/D_1$ is discussed below.

The remaining parameter values are essentially the same as those used in previous studies (Murray, 1974; Taylor and Murray, 1977). Recent measurements (Gayeski, 1981) indicate that the $P_{50}$ for dog myoglobin is 5.3 mm Hg, somewhat greater than previously reported. The total myoglobin concentration, $N_T$, is 0.5 mM, but calculations are done in the range of 0.01 mM to 1.0 mM. The dissociation velocity constant, $k = 66$ s$^{-1}$, is from Antonini and Brunori (1972) and is corrected to 37°C. A typical red muscle fiber has a radius of 25 $\mu$m and is surrounded by three to five capillaries (Honig et al., 1984). Oxygen consumption is set high, 15 ml $O_2$/100 g/min, to study maximal gradients and is assumed to be constant and uniform. It is realized that oxygen consumption decreases at low oxygen tensions because of Michaelis-Menten kinetics, but in this study the minimum oxygen tension in the fiber in all calculations presented remained above 0.5 mm Hg. In this range of oxygen tension, consumption is nearly constant. The parameters coming from bulk muscle measurements, $N_T$ and $M$, are adjusted for 10% extracellular mass in the muscle.

The relevant parameters and ranges are summarized in Table I in their most common units.

## RESULTS AND DISCUSSION

### General Results

The results presented in this study are displayed primarily as radial profiles of the oxygen tension, or some related quantity, from the sarcolemma, $r = R$, to the center of the muscle fiber, $r = 0$. Consider in Fig. 2 *A* some typical radial profiles of the oxygen tension (normalized by myoglobin $P_{50} = 5.3$ mm Hg) versus the normalized radial coordinate $r/R$, where zero is the center and unity is the sarcolemma of the fiber. The solid curves represent radial profiles along two distinct angular directions: $\theta_i$ where the capillaries are adjacent to the sarcolemma and the sarcolemmal oxygen tension is greatest ($P_{max}$); and $\theta_m^i$ where the midpoints between capillaries are located and the sarcolemmal oxygen tension is a minimum ($P_{min}$). Thus, the difference between the solid curves expresses the angular variation in oxygen tension, and it can be seen in Fig. 2 *A* that this difference is reduced rapidly away from the sarcolemma, $r/R = 1$. In subsequent discussions maximal angular variations in oxygen tension will be studied by looking at the ratio of these two curves, $P(r, \theta = \theta_i)/P(r, \theta = \theta_m^i)$, and maximal radial variations in oxygen tension will be studied by looking at $P(r, \theta = \theta_i)$.

The dashed curve in Fig. 2 *A* represents the oxygen tension profile calculated when the oxygen tension at the sarcolemma is uniform (no $\theta$ dependence) and equal to the average oxygen tension at the sarcolemma for the general $\theta$ dependent case. It is apparent that the oxygen tension profile based on a uniform, average oxygen tension surrounding the fiber predicts very accurately the oxygen tension in the core of the fiber. This occurs not only when the variation in oxygen tension at the sarcolemma, $P_s(\theta)$, is

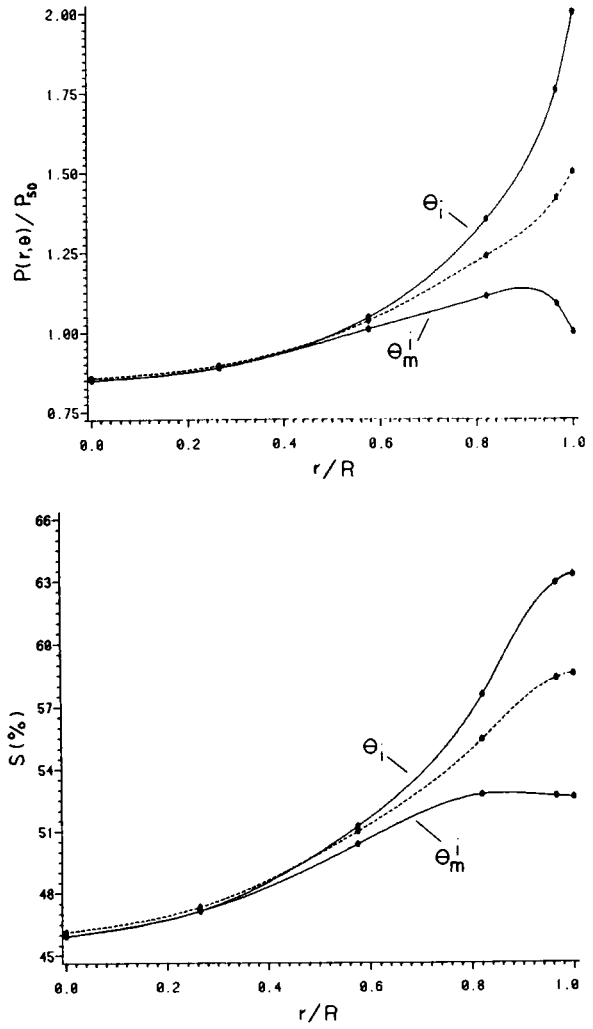


FIGURE 2 Typical radial profiles for normalized oxygen tension (*A*) and myoglobin saturation (*B*) in a muscle fiber. The solid curves represent the radial profiles at the $\theta_i$ and $\theta_m^i$ angular positions. The dashed curve is the radial profile based on a uniform oxygen tension at the sarcolemma which is the average of the sarcolemmal oxygen tension in the $\theta$ dependent case. All parameters assume their baseline values in Table I.

linear as in Fig. 2, but also for other variations in $P_s(\theta)$. For example, a sinusoidal variation in $P_s(\theta)$ between $P_{max}/P_{50} = 2$ and $P_{min}/P_{50} = 1$ leads to a normalized oxygen tension at the center of the fiber of 0.754; using the average sarcolemmal normalized oxygen tension for this case, which is 1.36, in the one-dimensional model leads to an oxygen tension in the center of 0.762. Similarly, a quadratic variation in $P_s(\theta)$ for the same values above produces a center oxygen tension (normalized) of 0.982; the average sarcolemmal oxygen tension in this case is 1.67, and in the one-dimensional model this sarcolemmal oxygen tension produces an oxygen tension at the center of the fiber of 0.989. Thus, the oxygen tension at the center of the fiber does depend on the nature of variation in $P_s(\theta)$ but is always nearly identical to that predicted from a one-dimensional model (no $\theta$ dependence) provided the uniform oxygen

tension at the sarcolemma is equal to the average sarcolemmal value in the $\theta$ dependent case. This result could have been anticipated from consideration of diffusion theory without facilitation effects.

In Fig. 2 *B* the corresponding myoglobin saturation, $S$, is displayed vs. radial position for the same case as in Fig. 2 *A*. Clearly, the angular variation of myoglobin saturation also does not persist into the fiber; the maximum angular variation in myoglobin saturation is <4% (saturation units) at $r/R = 0.8$. One can also notice that the slope of the radial profiles of oxymyoglobin saturation decreases to zero at the sarcolemma over a short distance. This thin oxymyoglobin boundary layer denotes the region where oxygen and myoglobin depart from equilibrium. Though there are different ways to characterize the departure from equilibrium in this boundary layer, one way is to compare the computed myoglobin saturation at the sarcolemma, $S(R, \theta)$, with the saturation value, $S_{eq}(R, \theta)$, that would be in equilibrium with the oxygen tension at the sarcolemma, $P(R, \theta)$. The equilibrium relationship ($T^* \rightarrow 0$ in Eq. 9) between oxygen and myoglobin is the hyperbolic curve: $S_{eq} = P/(P + P_{50})$. Table II compares the percent deviation of $S_{eq}(R, \theta)$ and $S(R, \theta)$ for $\theta = \theta_i$ (column three) as a function of the diffusion coefficients and the myoglobin concentration, $N_T$. These values represent the maximum departures from equilibrium found in this study, and as is apparent from Table II, the departures are small. Increasing the diffusion coefficients reduces the size of the non-equilibrium boundary layer (Murray, 1974), and as one would expect the departure from equilibrium decreases accordingly. The total myoglobin concentration, $N_T$, has only a small effect on the departure from equilibrium.

Table II also lists values for the percent facilitated transport under different conditions (column four). The fraction of facilitated transport is defined here as the ratio

TABLE II
PERCENT DEVIATION FROM EQUILIBRIUM* AND PERCENT FACILITATED TRANSPORT‡

| $D_l$ | $N_T$ | Percent deviation* | Percent facilitated transport‡ |
|---|---|---|---|
| 1.5 $D_{lb}$ | 0.5 mM | 5.20 | 50.2 |
| $D_{lb}$ | 0.5 mM | 5.40 | 52.5 |
| $D_{lb}/2$ | 0.5 mM | 6.58 | 60.1 |
| $D_{lb}/3$ | 0.5 mM | 8.08 | 66.8 |
| $D_{lb}$ | 0.05 mM | 5.02 | 16.1 |
| $D_{lb}$ | 0.1 mM | 5.04 | 25.6 |
| $D_{lb}$ | 0.25 mM | 5.16 | 41.0 |
| $D_{lb}$ | 1.0 mM | 5.92 | 62.3 |

All parameters, unless noted, assume their baseline values as given in Table I, and $D_{lb}$ denotes the baseline value for $D_l$ ($2 \times 10^{-5}$ cm$^2$s$^{-1}$). $D_2/D_l$ is fixed at 0.075.

*Percent deviation is defined in text as $[S_{eq}(R, \theta_i) - S(R, \theta_i)]/S(R, \theta_i) \times 100$.

‡Percent facilitated transport is defined in text as total inward flux of bound oxygen divided by the same flux of total oxygen, bound and free. Values in column four above are evaluated at $r/R = 0.57$.

of total inward flux of bound oxygen at a given radial position ($D_2\, \partial N_2/\partial r(r, \theta)$ integrated over $\theta$) divided by the total inward flux of all forms of oxygen, bound and free, at the same radial position ($D_l\, \partial N_l/\partial r(r, \theta) + D_2\, \partial N_2/\partial r(r, \theta)$ integrated over $\theta$). This fraction depends on the radial position, $r$, since both the free oxygen and bound oxygen gradients vary with $r$. Arbitrarily, the radial position, $r/R = 0.57$, is selected in Table II as a reference point for presenting some typical values. (This point is convenient since a collocation point is located there, see Appendix.) Apparently, the percent facilitation changes very little over the range of diffusion coefficients considered, with only a small shift towards more percent facilitation as diffusion coefficients decrease. Also, as one would expect the percent facilitation decreases with decreasing total myoglobin concentration. The decrease, however, is attenuated at higher myoglobin concentrations. Fletcher (1980) discusses in detail the spatial variation of percent facilitation in tissue.

It is worth commenting on the radial profile of oxygen tension in Fig. 2 *A* for $\theta = \theta_m^i$, where the oxygen tension at the sarcolemma is a minimum, $P_{min}$. Notice that the profile shows an outward flux of oxygen at the sarcolemma (reverse gradient) at this angular location. This may not be physiologically realizable and indicates that the selected variation in $P_s(\theta)$ may be too large, i.e. $P_{min}$ should be closer to $P_{max}$ than what we have considered. In fact, if a $P_{min}/P_{50}$ of 1.5 or greater is selected for the calculations of Fig. 2 *A* (rather than 1.0), the reverse gradient is eliminated. Thus, we may be considering angular variations in oxygen tension at the sarcolemma that are more severe than physiologically possible (i.e. a "worst-case" variation); however, in the following section it is shown that these "worst-case" variations do not persist significantly into the fiber under most physiological conditions, and hence the exact relationship between $P_{max}$ and $P_{min}$ is not crucial for studying gradients within the fiber.

## Angular Variations in Oxygen Tension

In this section maximum angular variations in oxygen tension are studied by looking at the ratio, $P(r, \theta = \theta_i)/P(r, \theta = \theta_m^i)$, under various conditions. This ratio is a convenient scale for studying angular variations in oxygen tension. As mentioned above, the angular variations in oxygen tension considered here may be "worst-case" variations compared to angular variations occurring in vivo. Consider Fig. 3 *A*, in which the effect of myoglobin concentration on maximum angular gradients is displayed. The four curves represent myoglobin concentrations of 0, 0.05, 0.1, and 0.5 mM; and the calculations are done for $C_f = 5$, $P_{max}/P_{50} = 2$, and $P_{min}/P_{50} = 1$. It is clear that the angular variations in oxygen tension decrease very rapidly away from the sarcolemma for all the myoglobin concentrations studied. In particular for fibers rich in myoglobin (0.5 mM), angular variations are less than 20% when $r/R = 0.8$.

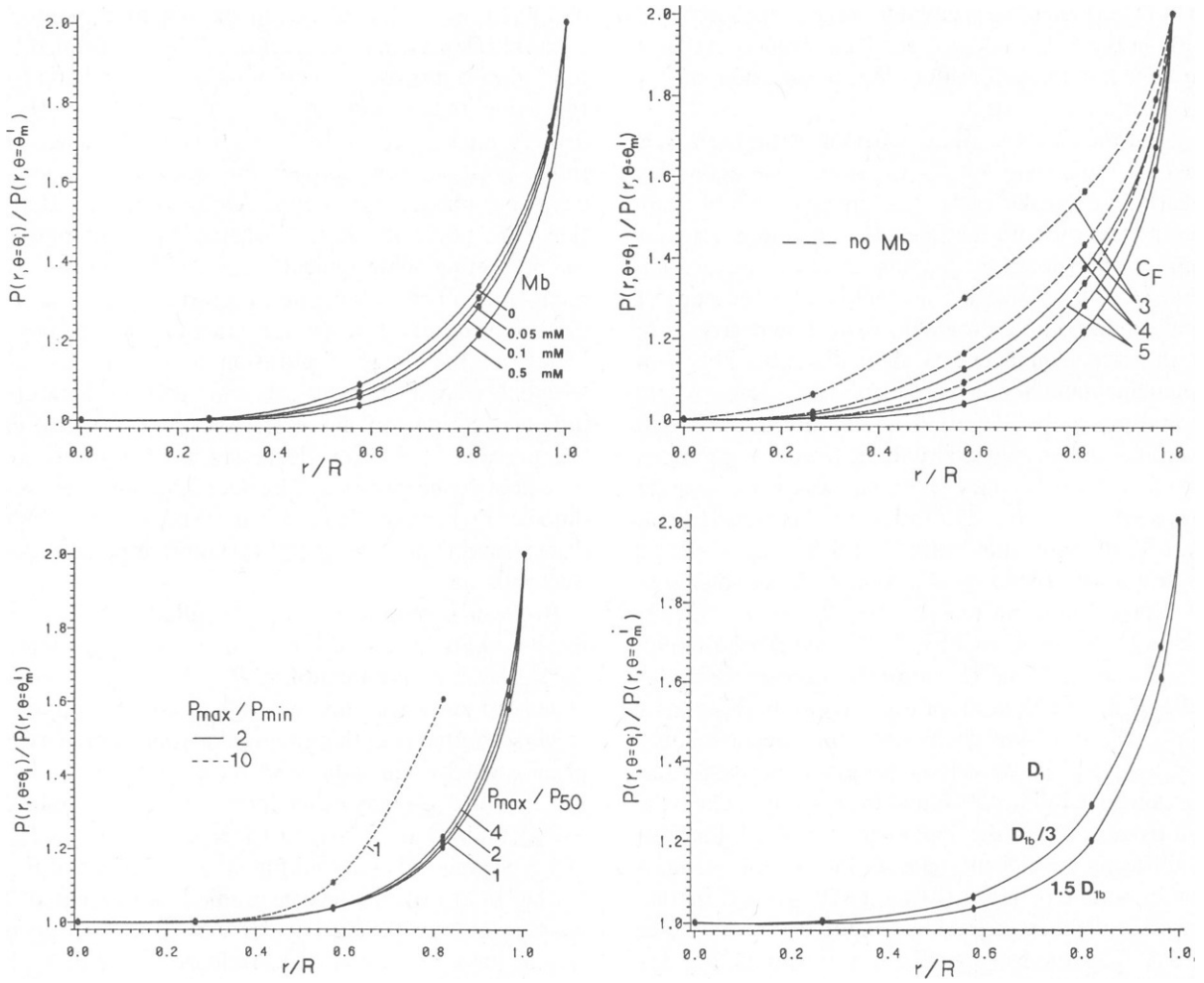


FIGURE 3 Angular variations of oxygen tension are studied by considering radial profiles of the ratio, $P(r, \theta = \theta_i)/P(r, \theta = \theta_m^i)$. The effects of myoglobin concentration ($A$), number of surrounding capillaries ($B$), oxygen tension at the sarcolemma ($C$), and diffusion coefficients ($D$) are presented. All parameters, except where noted, assume their baseline values in Table I. $D_{1b}$ refers to the baseline value for $D_1$ ($2 \times 10^{-5}$ $cm^2s^{-1}$) and $D_2/D_1$ is fixed (0.075).

A similar decrease in angular variations of oxygen tension occurs for different numbers of capillaries surrounding the fiber $C_f$. In Fig. 3 $B$ the solid curves denote the maximum angular variation in oxygen tension for $C_f$ = 3, 4, and 5, and a myoglobin concentration of 0.5 mM ($P_{max}$, $P_{min}$ same as in Fig. 3 $A$). The dashed curves represent the same cases as the solid curves but with no myoglobin facilitation. Except for the case of no myoglobin facilitation and only three surrounding capillaries, angular variations in oxygen tension do not persist deeply into the fiber. In this worst case angular variations are reduced to 20% at $r/R = 0.5$.

In Fig. 3 $C$ angular variations in oxygen tension are studied for several values of $P_{max}$ and $P_{min}$, with five capillaries surrounding the fiber and a 0.5 mM myoglobin concentration. The solid curves correspond to a ratio of $P_{max}/P_{min} = 2$, but for several different $P_{max}$ values. The dissipation of angular variations in oxygen tension is nearly independent of the selected value of $P_{max}$. This is significant because it is not known with certainty what the sarcolemmal oxygen tension level is in vivo; but from Fig. 3 $C$ some confidence is gained that angular variations in oxygen tension are dissipated quickly regardless. The dashed curve corresponds to a ratio of $P_{max}/P_{min} = 10$, undoubtedly an extreme value for oxygen tension variations on the sarcolemma of the fiber. In this case angular variations persist more deeply into the fiber than for smaller $P_{max}/P_{min}$ ratios; nevertheless, they are nearly eliminated at $r/R = 0.5$.

In Fig. 3 $D$ it is seen that dissipation of angular variations into the fiber does not depend significantly on the diffusion coefficients selected from the range of physiological values. Results are shown for the upper and lower $D_1$ values possible, $D_1 = 1.5\ D_{1b}$ and $D_1 = D_{1b}/3$, respectively, with $D_{1b} = 2 \times 10^{-5}$ $cm^2s^{-1}$. Recall that $D_2$ is also varied in Fig. 3 $D$ since the ratio, $D_2/D_1$, is taken to be a contant (0.075). Taken together, Figs. 3 $A$, 3 $B$, 3 $C$, and 3 $D$ indicate that for the geometry considered here angular variations in oxygen tension are of small concern since they

never persist deeply into the fiber. What is more important, as discussed above in relation to Fig. 2 *A*, is the average value of the sarcolemmal variations in oxygen tension. This value sets the oxygen tension in the core of the fiber.

A critical step in the modelling of oxygen gradients in this study was the choice for the boundary condition for the oxygen tension at the sarcolemma of the muscle fiber. Fortunately, the variation in oxygen tension imposed at the boundary does not penetrate deeply into the fiber since a priori we do not know the oxygen tension variation at the sarcolemma in vivo and must assume a simple boundary condition. For parameters relevant to dog gracilis muscle (0.5 mM myoglobin, $C_f$ is ~5), the dissipation of angular variations in oxygen tension occurs over a very short distance into the fiber, regardless of the value of $P_{max}$ or $P_{min}$. Furthermore, since angular variations in oxygen tension do not persist substantially into the fiber over a range of $C_f$ from 3 to 5, we can be confident that the assumption of equally-spaced capillaries is not a particularly limiting one; for the case, however, in which the surrounding capillaries are clustered completely at one edge of the sarcolemma, the results obtained here would not apply.

The calculations performed in this study assume that the surrounding capillaries are identical. If the oxygen tension in the surrounding capillaries is very different, we cannot draw any final conclusions about the dissipation of angular oxygen tension gradients. However, the results in Figs. 3 *A*,

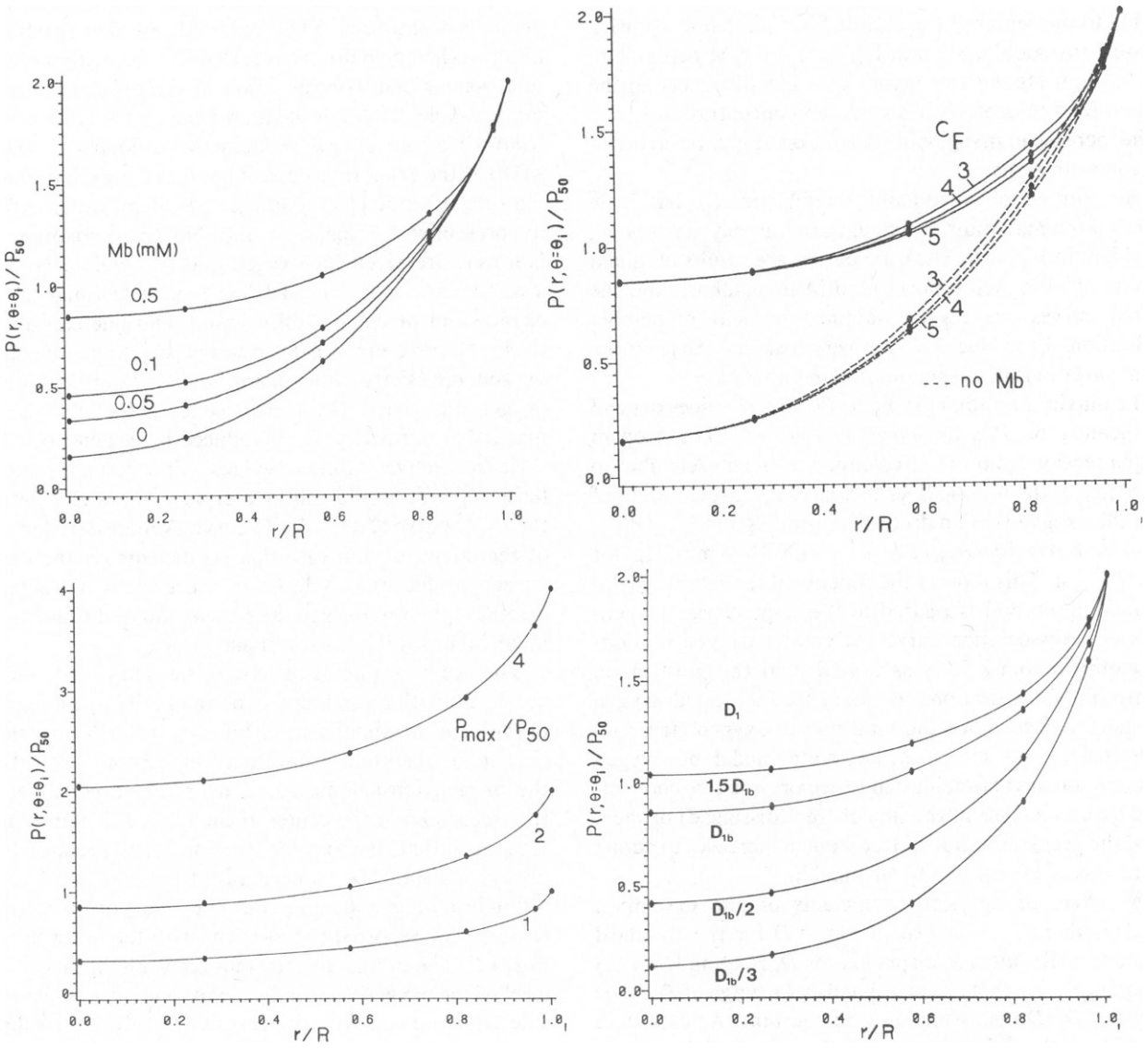


FIGURE 4 Maximal radial gradients of oxygen tension are studied by considering radial profiles of $P(r, \theta - \theta_1)$ normalized by $P_{50}$. The effects of myoglobin concentration (*A*), number of surrounding capillaries (*B*), oxygen tension at the sarcolemma (*C*), and diffusion coefficients (*D*) are presented. All parameters assume their baseline values in Table I, unless where noted. $D_{1b}$ is the baseline value for $D_1$, and $D_2/D_1$ is fixed.

3 *B*, 3 *C*, and 3 *D* leave us optimistic that angular variations of oxygen tension in this more complicated situation would also not persist deeply into the muscle fiber, especially for a myoglobin-rich muscle fiber like the dog gracilis.

## Radial Variations in Oxygen Tension

In this section maximal radial variations in oxygen tension are studied by looking at $P(r, \theta = \theta_i)$. Recall from Fig. 2 *A* that at the $\theta_i$ angular locations, where the capillaries are situated adjacent to the sarcolemma and the oxygen tension at the sarcolemma is $P_{max}$, the radial profile of oxygen tension is steepest. In Fig. 4 *A* the effect of myoglobin concentration on these radial profiles is shown. The results displayed in Fig. 4 *A* are for $C_f = 5$, $P_{max}/P_{50} = 2$, and $P_{min}/P_{50} = 1$. The drop in oxygen tension from the sarcolemma to the center of the muscle fiber is 6.1 mm Hg with 0.5 mM myoglobin, 8.2 mm Hg with 0.1 mM myoglobin, and 9.8 mm Hg with no myoglobin. The difference in the oxygen tension drop with myoglobin concentration is due to the increase in myoglobin facilitation at greater myoglobin concentrations.

The number of surrounding capillaries, $C_f$, has little effect on the maximum radial variation in oxygen tension, as evident in Fig. 4 *B*. The solid curves are results obtained with myoglobin facilitation (0.5 mM myoglobin), and the dashed curves are results obtained without myoglobin facilitation. The value of $C_f$ has very little influence on the radial variations in oxygen tension in either case.

The maximum radial gradient, $P(r, \theta = \theta_i)$, does depend significantly on $P_{max}$ as shown in Fig. 4 *C*. The drop in oxygen tension from the sarcolemma of the muscle fiber to the center of the muscle fiber increases for larger values of $P_{max}$: the oxygen tension drop is 3.7 mm Hg for $P_{max}/P_{50} = 1$, 6.1 mm Hg for $P_{max}/P_{50} = 2$, and 10.4 mm Hg for $P_{max}/P_{50} = 4$. This reflects the functional range of myoglobin facilitation and is related to the slope of the oxygen-myoglobin dissociation curve. At greater oxygen tensions myoglobin becomes fully saturated, and the gradient in oxymyoglobin saturation, necessary for facilitated oxygen transport, is lost. Since the total flux of oxygen (free and facilitated) is set in this steady-state model by oxygen consumption, loss of facilitated transport must be compensated by an increase in the flux of free (dissolved) oxygen. Thus, the gradient or flux of free oxygen increases to adjust for the loss of facilitation by myoglobin.

The effect of diffusion coefficients on the maximum radial gradient is displayed in Fig. 4 *D* for the standard parameters. Results are displayed for $D_1$ ranging from 1.5 $D_{1b}$ to $D_{1b}/3$, which also corresponds to a range of $D_2$ since the ratio, $D_2/D_1$, is assumed to be constant. As expected, the effect of the diffusion coefficient on the drop in oxygen tension from fiber periphery to core is significant: 5.1 mm Hg for 1.5 $D_{1b}$, 6.1 mm Hg for $D_{1b}$, 8.4 mm Hg for $D_{1b}/2$, and 10.0 mm Hg for $D_{1b}/3$. The increase in the oxygen tension drop, however, is less than linearly proportional to the decrease in diffusion coefficients, e.g. a halving of the diffusion coefficients, from $D_{1b}$ to $D_{1b}/2$ increases the oxygen tension drop from fiber periphery to core by only 38%. This attenuating effect is due to the presence of myoglobin facilitation; without myoglobin the oxygen tension drop would be linearly and inversely proportional to the diffusion coefficient for oxygen.

At this point it is worth addressing the assumption of a constant ratio for $D_2/D_1$. This assumption was necessary because of a lack of detailed experimental data in the literature for myoglobin diffusion in tissue and a lack of data directly addressing the oxygen and myoglobin diffusivity dependence in various media. The diffusivity ratio is likely to depend on the medium considered. Spaan et al. (1980) provide some data for oxygen and hemoglobin diffusivities in hemoglobin solutions of varying total hemoglobin concentration. Their data indicate that the diffusivity ratio (hemoglobin to oxygen) decreases with increasing total hemoglobin concentration of the diffusing medium. For example, doubling the total hemoglobin concentration from 10 g% to 20 g% reduces the ratio from ~0.02 to ~0.015 (the exact ratios are difficult to determine from the semi-logarithmic plots of oxygen and hemoglobin diffusivity presented by Spaan et al.). No corresponding data, however, are given for oxygen and myoglobin. Nonetheless, the results in Fig. 4 *D* cover a wide range of both oxygen and myoglobin diffusivities, and one can qualitatively interpret Fig. 4 *D* for cases in which the myoglobin-oxygen diffusivity ratio changes. For example, suppose oxygen diffusivity, $D_1$, is reduced by a factor of 2 while myoglobin diffusivity, $D_2$, is reduced by a factor of 3 from their respective baseline values. The resultant oxygen tension profile would fall in Fig. 4 *D* somewhere between the $D_{1b}/2$ curve and the $D_{1b}/3$ curve. A more detailed study of the effect of both diffusion coefficients on the oxygen tension profile in muscle fibers must await more experimental data on oxygen and myoglobin diffusivities in identical or similar muscle tissue in situ.

The radial gradients of oxygen tension in Fig. 4 *C* are consistent with those found experimentally by Honig et al. (1984) for maximally-respiring dog gracilis muscle. In particular, they find a difference of <2 mm Hg between the oxygen tension measured near the sarcolemma and that measured at the center of the fiber. It is important to recognize that the oxygen tension they measured was always <3 mm Hg (a normalized value of ~0.6 on the ordinate of Fig. 4 *C*, and thus the small drop in oxygen tension they reported is consistent with the lower curve in Fig. 4 *C*. The drop in oxygen tension would be larger if the level of the oxygen tension in the muscle fiber is increased. The arguments above assume that the diffusion coefficient for oxygen in dog gracilis is near or above the baseline value, $D_{1b} = 2 \times 10^{-5}$ cm$^2$s$^{-1}$. Since the oxygen diffusion coefficient has never been reported for this muscle we can only speculate that this is true. It is interesting, however, that the in-situ measurements of oxygen diffusion coeffi-

cients by Ellsworth and Pittman (1984) on different hamster muscles show that the 100% oxidative soleus muscle had the largest oxygen diffusion coefficient, which is larger than $D_{1b}$ in this study. Also, as pointed out by Jacquez (1984), the local temperature in a heavily exercising muscle may exceed 37°C by several degrees and this would act to increase diffusion coefficients.

## The Minimum Average Sarcolemmal Oxygen Tension

The important effect of myoglobin concentration on oxygen tension gradients is summarized in this section by defining the minimum average oxygen tension at the sarcolemma. Recall from the discussion in General Results that the oxygen tension in the core of the fiber can be predicted well by assuming a uniform oxygen tension at the sarcolemma that is the average of the oxygen tension along the sarcolemma in the general two-dimensional case for any reasonable variation in $P_s(\theta)$. To proceed, then, we define the minimum average oxygen tension at the sarcolemma to be the minimum value of the uniform oxygen tension at the sarcolemma such that anoxia does not occur at the center of the fiber. Clearly the distinction between anoxia and normoxia is not precise, so as a working definition we week the value of the uniform sarcolemmal oxygen tension that leads to a normalized oxygen tension at the center of the fiber of 0.1, or ~0.5 mm Hg in dimensional terms.

This minimum average sarcolemmal oxygen tension, $\hat{P}_{min}$, is displayed in Fig. 5 as a function of the total myoglobin concentration of the muscle fiber for $M_{max}$ = 15 ml $O_2$/100 g/min. Values are given for the complete physiological range of diffusion coefficients considered in this study. Above a myoglobin concentration of 0.5 mM the minimum average oxygen tension at the sarcolemma becomes less sensitive to the diffusion coefficients selected and is <5 mm Hg over most the range for diffusion coefficients. Of real significance for maximally-respiring muscle fibers is the drop in the minimum average oxygen tension at the sarcolemma that occurs when the myoglobin concentration increases above 0.1 mM. The substantial drop is caused by the additive nature of two factors discussed previously: myoglobin-facilitated transport is greater with increasing myoglobin concentration (more oxygen carrier is available); and as oxygen tensions become lower, the functional range for myoglobin is realized (myoglobin becomes more desaturated) and myoglobin facilitation increases. The increase in myoglobin-facilitated oxygen transport means that oxygen consumption, which sets the total oxygen transport rate (free and facilitated), is satisfied with less transport of free oxygen; thus the oxygen tension gradient from sarcolemma to center is smaller.

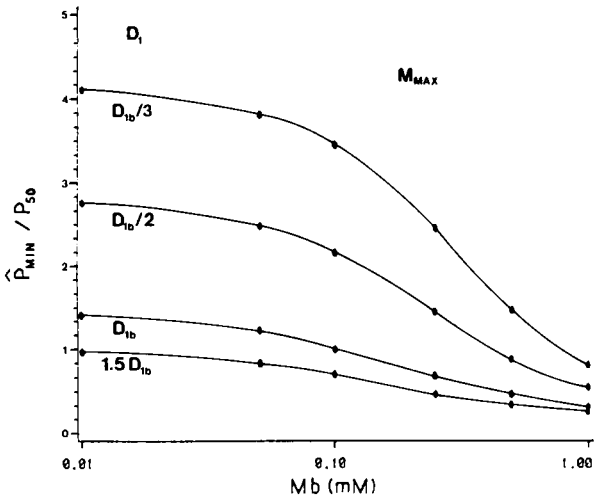


FIGURE 5 Minimum average sarcolemmal oxygen tension as defined in The Minimum Average Sarcolemmal Oxygen Tension normalized by $P_{50}$ vs. myoglobin concentration for maximal oxygen consumption. Curves correspond to different diffusivities, where $D_{1b} = 2 \times 10^{-5}$ cm$^2$s$^{-1}$ and $D_2/D_1$ is fixed at 0.075. All other parameters as defined in Table I.

The results in Fig. 5 can aid in the interpretation of experiments in which myoglobin function is abolished in intact working skeletal muscles. Cole (1982) eliminated functional myoglobin in the dog gastrocnemius-plantaris muscle by using hydrogen-peroxide to convert myoglobin to higher oxidation states incapable of binding oxygen. He found that twitch tension and oxygen consumption were reduced significantly as compared to control animals, suggesting (but not establishing) that the muscle fibers became hypoxic when myoglobin function was abolished. The oxygen consumption in Cole's experiments corresponded roughly to one-half the maximal value used in Fig. 5. From Fig. 5, abolishing myoglobin at maximal consumption leads to a minimum average sarcolemmal oxygen tension of ~7 mm Hg (ordinate intercept in Fig. 5) for $D_1 = D_{1b}$. At half-maximal consumption this number is probably around 3 to 5 mm Hg, a very low value when compared with the oxygen tension one would expect in capillary blood. Thus, either the muscle fibers in Cole's experiments did not become hypoxic when myoglobin was abolished, and twitch tension was compromised for some other reason; or the fibers did become hypoxic, and the average oxygen tension at the sarcolemma was very low, on the order of 3 to 5 mm Hg. The latter would suggest that capillary blood has either a low oxygen tension (significant precapillary losses of oxygen occur), and/or the oxygen tension drop from inside the capillaries to the sarcolemma is very large. Studies of Katz et al. (1984) on cardiac myocytes suggest that a large drop in oxygen tension from capillaries to sarcolemma may in fact occur.

## SUMMARY AND COMMENT

An important finding of the present modeling study is that the variation in the oxygen tension along the sarcolemma (periphery) of a skeletal muscle fiber does not penetrate

substantially into the fiber, especially for parameters relevant to myoglobin-rich red muscle (0.5 mM myoglobin). The relatively quick dissipation of angular variations of oxygen tension into the fiber is significant for the model. Primarily, it justifies the model boundary condition for oxygen tension at the sarcolemma of the muscle fiber. As a first approximation, there is little need for treating this boundary condition in a more complex manner. The oxygen tension in the majority of the muscle fiber is determined mainly by the average oxygen tension at the sarcolemma and not by sarcolemmal variations of the oxygen tension. The results discussed above are not unexpected if one considers diffusion theory without facilitation effects. The presence of myoglobin merely reduces somewhat the depth to which angular variations at the sarcolemma penetrate without myoglobin.

Though earlier studies have addressed the role of myoglobin in red skeletal muscle fibers, the strong specific effect of myoglobin concentration viewed in terms of a minimum average sarcolemmal oxygen tension has not been reported. A myoglobin-rich skeletal muscle fiber with a myoglobin concentration greater than 0.1 mM can sustain very high oxygen consumptions with a surrounding average oxygen tension of ~4 mm Hg or less if diffusion coefficients are in the upper portion of the physiological range. Above a myoglobin concentration of 0.5 mM, the minimum average sarcolemmal oxygen tension is below 5 mm Hg over a large range of diffusion coefficients. The results of this model study show that the existence of flat, shallow gradients of oxygen tension in red muscle fibers is consistent with theoretical considerations of oxygen diffusion and consumption rates in this tissue, and that the magnitude of these oxygen gradients depends strongly on the myoglobin concentration and oxygen tension level of the muscle fibers.

## APPENDIX

## Numerical solution of transport equations

The transport equations, Eqs. 7 and 8, are solved subject to the boundary conditions, Eqs. 10 and 11, using a mix of numerical techniques. The character of the transport equations leads to a thin boundary layer region near the muscle sarcolemma, $r = R$. In this thin boundary layer region the reaction between oxygen and myoglobin departs from chemical equilibrium, and reaction rates become comparable to diffusion rates. Outside of this boundary layer oxygen and myoglobin are in equilibrium. The existence of these type of boundary layers has been well studied for the oxygen-myoglobin problem (see Murray, 1974; Fletcher, 1980) and have been exploited to obtain an approximate analytical solution to the transport equations in one spatial dimension using techniques such as matched asymptotic expansions. In the present study, however, the two spatial dimensions complicates the problem sufficiently that, although a asymptotic solution may be obtainable, it is easier to solve the full transport equations directly by numerical techniques.

It is imperative that the numerical techniques resolve sufficiently the nonequilibrium boundary layer region. Murray (1974) calculates that the thickness of the boundary layer is on the order of 1 $\mu$m or less and hence the spatial resolution of the numerical scheme in the radial direction should be relatively fine. In this study the transport equations are discretized in the $r$ direction using orthogonal collocation (see Finlayson, 1980, for a good description of all the numerical techniques discussed below) and in the $\theta$ direction using standard finite differences.

As an example, the discretization of the free oxygen transport equation, Eq. 7, is described. The $r, \theta$ space in the muscle fiber is divided into radial collocation points located along angular rays. Let $r_i$ be the $i$th radial collocation point (in the subsequent discussion the radial coordinate has been normalized by muscle fiber radius, $R$, so that $0 \le r_i \le 1$) and $\theta_j$ be the $j$th angular finite difference ray. We denote the $(r_i, \theta_j)$ spatial point by $ij$, $P(r_i, \theta_j)$ by $P_{ij}$, and $T^*(r_i, \theta_j)$ by $T^*_{ij}$ for simplicity, where $T^*_{ij}$ is a function of $P_{ij}$ and $S_{ij}$ from Eq 9. The fundamental step in the discretization is approximating $\nabla^2 P$ at the $ij$ spatial point by a discrete form, where $\nabla^2 = 1/R^2[1/r\,\partial/\partial r(r\partial/\partial r) + 1/r^2\,\partial^2/\partial\theta^2]$. The angular part of $\nabla^2 P$ at $ij$ is approximated using finite differences:

$$\partial^2 P/\partial\theta^2 = (P_{ij+1} - 2P_{ij} + P_{ij-1})/\Delta\theta^2, \tag{A1}$$

where $\Delta\theta$ is the angular difference between adjacent rays. The approximation for the radial part of $\nabla^2 P$ is obtained as follows (see Finlayson, 1980, pp. 94–97). The $r$ dependence of $P(r, \theta)$ is expanded in polynomials of $r^2$ due to the radial symmetry of the problem:

$$P(r, \theta) = \sum_{k=1}^{N+1} d_k r^{2k-2}, \tag{A2}$$

where $d_k$ are unknown factors depending on $\theta$, and $N$ is the number of interior ($r < 1$) radial collocation points chosen. From Eq. A2 the value of $P_{ij}$ is given by $P(r_i, \theta_j)$:

$$P_{ij} = \sum_{k=1}^{N+1} d_{kj} r_i^{2k-2}, \tag{A3}$$

where $d_{kj}$ is a short way to write $d_k(\theta_j)$. Also using Eq. A2, the radial part of $\nabla^2 P\,(1/r\,\partial/\partial r(r\partial P/\partial r)$ can be calculated explicitly and then evaluated at the $ij$ spatial point. This quantity is denoted $U_{ij}$ and is given by

$$U_{ij} = \sum_{k=1}^{N+1} d_{kj}\,(2k - 2)^2 r_i^{2k-4}. \tag{A4}$$

At this step it is useful to introduce vector notation: let $\boldsymbol{P}_j$ be the vector of $P_{ij}$ values from $i = 1$ to $N + 1$, $\boldsymbol{d}_j$ be the vector of unknown factors $d_{kj}$ from $k = 1$ to $N + 1$, and $\boldsymbol{U}_j$ be the vector of radial derivatives $U_{ij}$ from $i = 1$ to $N + 1$. Then Eqs. A3 and A4, respectively, can be written as

$$\boldsymbol{P}_j = \boldsymbol{Q}\,\boldsymbol{d}_j; \tag{A5}$$

$$\boldsymbol{U}_j = \boldsymbol{D}\,\boldsymbol{d}_j, \tag{A6}$$

where $\boldsymbol{Q}$ and $\boldsymbol{D}$ are matrices whose elements depend only on the values of the radial collocation points viz. $Q_{ik} = r_i^{2k-2}$ and $D_{ik} = (2k - 2)^2 r_i^{2k-4}$. From Eq. A5 it is apparent that $\boldsymbol{d}_j = \boldsymbol{Q}^{-1}\boldsymbol{P}_j$, where $\boldsymbol{Q}^{-1}$ denotes the inverse of $\boldsymbol{Q}$. Thus, the radial part of $\nabla^2 P$ at $ij$ can be rewritten as

$$\boldsymbol{U}_j = \boldsymbol{D}\,\boldsymbol{Q}^{-1}\,\boldsymbol{P}_j = \boldsymbol{B}\,\boldsymbol{P}_j, \tag{A7}$$

where the matrix $\boldsymbol{B} = \boldsymbol{D}\boldsymbol{Q}^{-1}$ depends only on the collocation points selected (i.e. the $r_i$), which will be discussed below. Once the elements of $\boldsymbol{B}$ are calculated, Eq. A7 can be resolved into its components:

$$U_{ij} = \sum_{k=1}^{N+1} B_{ik} P_{kj}, \tag{A8}$$

which is the desired approximation to the radial derivative at the $ij$ spatial point. The discretized form of the free oxygen transport equation, Eq. 7 is

$$0 = \alpha D_1/R^2\left[\left(\sum_{k=1}^{N+1} B_{ik}P_{kj}\right) + 1/(r_i^2\Delta\theta^2)\,(P_{ij+1} - 2P_{ij} + P_{ij-1})\right] - T^*_{ij} - M, \tag{A9}$$

which is an algebraic equation for the $P_{ij}$ and is applied to all the interior $ij$ spatial points. The $i = N + 1$ radial collocation point is the boundary $r = 1$. In a similar manner other necessary quantities, e.g. first derivatives, can be calculated. The discretization of the oxymyoglobin transport equation, Eq. 8, proceeds similarly. The discretized transport equations applied to the interior $ij$ spatial points in combination with the applicable boundary conditions provide simultaneous algebraic equations for all the unknown $P_{ij}$ and $S_{ij}$. These algebraic equations are solved in an iterative manner using the method of successive over-relaxation (see Finlayson, 1980, pp. 280–281).

The values of the $r_i$ radial collocation points that are necessary to obtain the elements of $\boldsymbol{B}$ are chosen as the zeroes of orthogonal polynomials. These polynomials are generated in cylindrical $r$ space using the following orthogonality constraint:

$$\int_{r=0}^{r=1} Y_k(r^2)\, Y_m(r^2)\, r dr = 0 \quad k \leq m - 1,$$

where $Y_k$ is a polynomial of degree $k$ in $r^2$. For a given $N$ the interior collocation points, $r_1 \ldots r_N$, are the zeroes of the $Y_N$ polynomial constructed above. The rationale for this manner of choosing the $r_i$ is beyond the scope of the Appendix but can be found in Finlayson (1980), where tables of the $r_i$ values can also be found. For $N = 4$, the points are (to two digits): $r_1 = 0.26$, $r_2 = 0.57$, $r_3 = 0.82$, $r_4 = 0.96$, and as always $r_{N+1} = 1$.

The resolution of the discretization must be increased (i.e. more finite difference grids in the $\theta$ direction and more collocation points in the $r$ direction) until the solution converges within a specified criterion. In the $\theta$ direction, 20 finite difference grids from $\theta_i$ to $\theta_m^i$ were found to be more than sufficient for accurate results. To demonstrate convergence with increasing resolution in the radial direction a typical calculation for the oxygen tension profile in the muscle fiber at $\theta = \theta_i$ is displayed in Fig. 6 for various number of radial collocation points, $N = 2$, 3, 4, 5, and 6. The exact ordinate intercept values ($r/R = 0$) for $N = 4$, 5, and 6 were hard to label for this figure because the values were nearly equal; the actual values are 0.856 for $N = 4$, 0.861 for $N = 5$, and 0.863 for $N = 6$. The curve for $N = 4$ corresponds to the calculations displayed in Fig. 2 *A*. It is clear from Fig. 6 that $N = 4$ represents a reasonable level of accuracy in the calculations for the type of results presented in this study. It is important to point out that the radial collocation points are not evenly spaced and with $N = 4$ the point, $r_4 = 0.965$, is within 0.875 $\mu$m of the sarcolemma for a 25 $\mu$m radius muscle fiber. Thus, the $r_4$ collocation point lies within the boundary layer region, which is ~1 $\mu$m thick (as discussed above). Fig. 6 leads us to the conclusion that for reasonably accurate calculation of the oxygen profiles presented in this study one collocation point inside the boundary layer is sufficient.

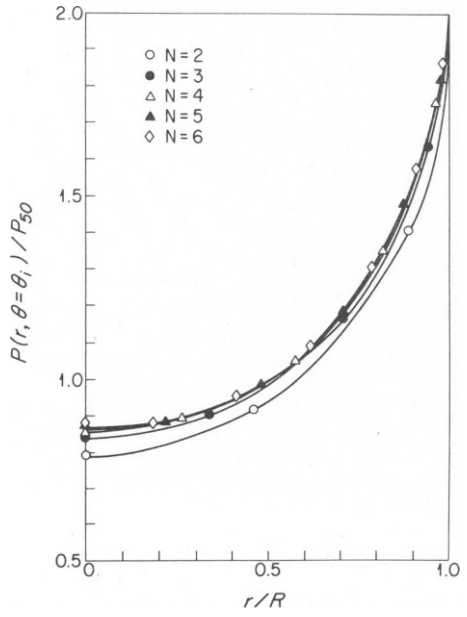


FIGURE 6 Convergence of numerical calculation of oxygen tension profiles with increasing number of radial collocation points, $N$.

The efficacy of orthogonal collocation in reaction-diffusion problems is not a new finding of this study. Federspiel (1983) looked at a similar problem of oxygen transport in hemoglobin solutions and found that $N = 3$ orthogonal collocation points in the domain gave the same results as using 40 finite difference grids. Eilbeck (1983) looked at general reaction-diffusion problems using a collocation procedure that was slightly improved over the one used in this study; he found that eight collocation points gave identical results as 720 finite difference grids. Finlayson (1980, pp. 98–104) also gives several comparisons between orthogonal collocation and finite differences that demonstrate the accuracy and efficiency of collocation vs. finite differences.

The author wishes to thank Drs. C. R. Honig and T. E. J. Gayeski for many helpful discussions of the problem, Dr. A. S. Popel for his helpful comments on the manuscript, and Ms. Alice Zilcha for typing the manuscript. The assistance of The Biomechanics Institute in the final stages of manuscript completion is also appreciated.

The work was supported by National Institutes of Health grants HL 33172 and HL 18292.

*Received for publication 15 November 1985 and in final form 18 February 1986.*

## REFERENCES

Antonini, E., and M. Brunori. 1971. *Hemoglobin and Myoglobin in their Reactions with Ligands*. Elsevier/North Holland, New York.

Cole, R. P. 1982. Myoglobin function in exercising skeletal muscle. *Science (Wash. DC)*. 216:523–525.

Eilbeck, J. C. 1983. A collocation approach to the numerical calculation of simple gradients in reaction-diffusion systems. *J. Math. Biol.* 16:233–249.

Ellsworth, M. J. and R. N. Pittman. 1984. Heterogeneity of oxygen diffusion through hamster striated muscles. *Am. J. Physiol.* 246:H161–H167.

Federspiel, W. J. 1983. Engineering analysis of two blood transport problems. Ph.d. dissertation, University of Rochester, Rochester, NY. 326 pp.

Finlayson, B. A. 1980. Nonlinear Analysis in Chemical Engineering. McGraw-Hill, Inc., NY. 366 pp.

Fletcher, J. E. 1980. On facilitated oxygen diffusion in muscle tissues. *Biophys. J.* 29:437–458.

Gayeski, T. 1981. A cryogenic microspectrophotometric method for measuring myoglobin saturation in subcellular volumes; application to resting dog gracilis muscle. Ph.D. dissertation, University of Rochester, Rochester, NY.

Gayeski, T. E. J., and C. R. Honig. 1983. Direct measurement of intracellular $O_2$ gradients; role of convection and myoglobin. *Adv. Exp. Med. Biol.* 159:613–621.

Goldstick, T. K., V. T. Ciuryla, and L. Zuckerman. 1975. Diffusion of oxygen in plasma and blood. *Adv. Exp. Med. Biol.* 75:183–190.

Honig, C. R., T. E. J. Gayeski, W. J. Federspiel, A. Clark, Jr., and P. Clark. 1984. Muscle $O_2$ gradients from hemoglobin to cytochrome; new concepts, new complexities. *Adv. Exp. Med. Biol.* 169:23–38.

Jacquez, J. A. 1984. The physiological role of myoglobin: more than a problem in reaction-diffusion kinetics. *Math. Biosci.* 68:57–97.

Jones, D. P., and F. G. Kennedy. 1982. Intracellular $O_2$ gradients in cardiac myocytes; lack of a role for myoglobin in facilitation of intracellular $O_2$ diffusion. *Biochem. Biophys. Res. Commun.* 105:419–424.

Katz, I. R., J. B. Wittenberg, and B. A. Wittenberg. 1984. Monoamine oxidase, an intracellular probe of oxygen pressure in isolated cardiac myocytes. *J. Biol. Chem.* 259:1504–1509.

Kawashiro, T., W. Nusse, and P. Scheid. 1975. Determination of diffusivity of oxygen and carbon dioxide in respiring tissue: results in rat skeletal muscle. *Pflugers Arch. Eur. J. Physiol.* 359:231–251.

Koning, J., L. J. C. Hoofd, and F. Kreuzer. 1981. Oxygen transport and the function of myoglobin; theoretical model and experiments in chicken gizzard smooth muscle. *Pflugers Arch. Eur. J. Physiol.* 389:211–217.

Kreuzer, F. 1970. Facilitated diffusion of oxygen and its possible significance; a review. *Respir. Physiol.* 9:1–30.

Livingston, D. J., G. N. LaMar, and W. D. Brown. 1983. Myoglobin diffusion in bovine heart muscle. *Science (Wash. DC).* 220:71–73.

MacDougall, J. D. B., and M. McCabe. 1967. Diffusion coefficient of oxygen through tissues. *Nature (Lond.).* 215:1173–1174.

Murray, J. D. 1974. On the role of myoglobin in muscle respiration. *J. Theor. Biol.* 47:115–126.

Riveros-Moreno, V., and J. B. Wittenberg. 1972. The self-diffusion coefficients of myoglobin and hemoglobin in concentrated solutions. *J. Biol. Chem.* 247(3):895–901.

Snell, F. M. 1965. Facilitated transport of oxygen through solutions of hemoglobin. *J. Theor. Biol.* 8:469–479.

Spaan, J. A. E., F. Kreuzer, and F. K. van Wely. 1980. Diffusion coefficients of oxygen and hemoglobin as obtained simultaneously from photometric determination of the oxygenation of layers of hemoglobin solutions. *Pflugers Arch. Eur. J. Physiol.* 384:241–251.

Taylor, B. A., and J. D. Murray. 1977. Effect of the rate of oxygen consumption on muscle respiration. *J. Math. Biol.* 4:1–20.

Van Ouwerkerk, H. J. 1977. Facilitated diffusion in a tissue cylinder with an anoxic region. *Pflugers Arch. Eur. J. Physiol.* 372:221–230.

Wittenberg, B. A., J. B. Wittenberg, and P. R. B. Caldwell. 1975. Role of myoglobin in the oxygen supply to red skeletal muscle. *J. Biol. Chem.* 250:9038–9043.

Wittenberg, J. B. 1970. Myoglobin-facilitated oxygen diffusion: role of myoglobin in oxygen entry into muscle. *Physiol. Rev.* 50:559–636.

Wyman, J. 1966. Facilitated diffusion and the possible role of myoglobin as a transport mechanism. *J. Biol. Chem.* 241:115–121.